Environmental Pollution 374 (2025) 126202

Contents lists available at ScienceDirect

Environmental Pollution

journal homepage: www.elsevier.com/locate/envpol

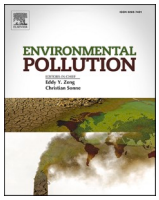

Sulfidated zero-valent iron bimetals for passive remediation of chlorinated vapors in the subsurface☆

Clarissa Settimi, Daniela Zingaretti *, Iason Verginelli, Renato Baciocchi

Department of Civil Engineering and Computer Science Engineering, University of Rome "Tor Vergata", Via del Politecnico 1, 00133, Rome, Italy

ARTICLE INFO

Keywords:
Zero-valent iron
Sulfidation
Bimetal
Dechlorination
Chlorinated solvents vapors
Risk mitigation strategies

ABSTRACT

This study explores a novel application of sulfidated zero-valent iron (S-ZVI) bimetals for the treatment of chlorinated solvents in the vapor phase. The potential of these reactive materials was investigated through batch, column, and modeling tests. The materials were produced by disc milling of ZVI, sulfur (S), copper (Cu), and nickel (Ni) with molar ratios of 0.05 and 0.2. The reactivity of the materials was assessed through vapor degradation batch tests conducted under partially saturated conditions using trichloroethylene (TCE) as a model compound. Sulfidated materials with a 0.05 S/ZVI molar ratio were the most reactive, achieving up to 99 % degradation of TCE vapors within 18 h and first-order degradation constants of 5–5.7 d^{-1}. Compared to the non-sulfidated materials, sulfidated ones remained reactive even after aging by exposure to air for 30 days. In all tests, C_3-C_6 hydrocarbons were detected as main byproducts, indicating β-elimination as the dominant TCE degradation pathway, with minor dichloroethylene and vinyl chloride amounts from the hydrogenolysis pathway. To evaluate the use of sulfidated bimetals as Horizontal Permeable Reactive Barriers (HPRBs) for treating chlorinated vapors in the subsurface, TCE diffusion column tests were performed using a 5 cm thick reactive layer of S-ZVI-Ni. These tests demonstrated up to 70 % degradation over 25 days. By integrating the column test results into an analytical model, it was estimated that an 18 cm HPRB could ensure up to 99 % degradation of TCE vapors. These findings highlight the potential of S-ZVI bimetals as an effective passive mitigation system for reducing chlorinated solvent vapor emissions from the subsurface.

1. Introduction

Zero-valent iron (ZVI) has long been known as an effective material for degrading chlorinated solvents, such as trichloroethylene (TCE), in groundwater (Phillips et al., 2010; ITRC, 2011; Fu et al., 2014). Namely, ZVI can induce the degradation of such compounds by reductive dechlorination, involving the substitution of chlorine atoms with hydrogen ones until obtaining the conversion into less harmful compounds (Arnold and Roberts, 2000; Liu et al., 2005; Phillips et al., 2010). In the remediation of sites impacted by chlorinated solvents, ZVI is commonly used as filling material for vertical permeable reactive barriers (PRBs) to treat contaminated groundwater (McCarty, 2010; ITRC, 2011; Fan et al., 2017; Gu et al., 2019). However, chlorinated solvents could volatilize from groundwater in the unsaturated zone at contaminated sites, potentially causing vapor intrusion into buildings (Verginelli et al., 2017; Ma et al., 2020). To mitigate vapor intrusion risks, horizontal permeable reactive barriers (HPRBs) have been suggested as a passive mitigation strategy aimed at addressing the contaminated vapors plume arising from the source of contamination to buildings (Mahmoodlu et al., 2014, 2015; Verginelli et al., 2017; Zingaretti et al., 2020; Settimi et al., 2023; Wang et al., 2024; Zhu et al., 2024). To realize these barriers, ZVI was proposed as a filling material and recently tested for the degradation of TCE vapors (Zingaretti et al., 2019, 2020).

In permeable reactive barriers, the use of micrometric ZVI is preferable to avoid particle aggregation issues compared to nanometric (Zingaretti et al., 2020; Settimi et al., 2022). However, micrometric ZVI generally shows lower reactivity towards dechlorination due to its limited surface area (He et al., 2018). For this reason, several modification techniques have been proposed to enhance ZVI reactivity towards the degradation of chlorinated compounds (Rajajayavel and Ghoshal, 2015; Gu et al., 2017; Xiao et al., 2022; Fan et al., 2016). One of these involves the addition of secondary metals, such as copper (Cu) or nickel (Ni), on ZVI particles forming bimetals (Kim and Carraway, 2003; O'Carroll et al., 2013; Scaria et al., 2020; Tian et al., 2022). Namely, Cu

☆ This paper has been recommended for acceptance by Charles Wong.

* Corresponding author.
E-mail address: zingaretti@ing.uniroma2.it (D. Zingaretti).

https://doi.org/10.1016/j.envpol.2025.126202
Received 30 January 2025; Received in revised form 17 March 2025; Accepted 2 April 2025
Available online 3 April 2025

forms a galvanic couple with ZVI, thus accelerating electron transfer and enhancing the dechlorination reactions (Liu et al., 2017; He et al., 2018; Settimi et al., 2023; Yang et al., 2023). Instead, Ni promotes both electron transfer and molecular hydrogen (H_2) dissociation into atomic hydrogen (H*), necessary for replacing chlorine atoms in chlorinated compounds molecules during dechlorination (Schrick et al., 2002; Kim and Carraway, 2003; Xu et al., 2012; Ruan et al., 2019; Settimi et al., 2022). ZVI bimetals have been widely studied for the degradation of chlorinated compounds in the aqueous phase (Kim and Carraway, 2003; Xu et al., 2012; Liu et al., 2017; Venkateshaiah et al., 2022; He et al., 2018). However, few studies involved their use as reagents for dechlorination in the vapor phase (Grenier et al., 2004; Settimi et al., 2022, 2023).

Despite their efficacy in degrading chlorinated solvents, ZVI and ZVI bimetals could be subjected to passivation, i.e., the formation of oxide layers on the particles surface, which inhibits electron transfer, consequently reducing the long-term reactivity of the materials (Gu et al., 2017; He et al., 2018; Gong et al., 2020; Fan et al., 2023a; Yan et al., 2024; Guan et al., 2015; Han and Yan, 2016). In this context, sulfidation has been proposed as a modification technique for ZVI. Sulfidation refers to the addition of sulfur to ZVI, forming iron sulfide phases (e.g., FeS) on the surface of the particles (Cai et al., 2021). This modification increases ZVI reactivity and selectivity for chlorinated compounds degradation and, in parallel, promotes the treatment longevity by reducing passivation (Gu et al., 2019; Xu et al., 2019; Zou et al., 2019; Gong et al., 2020; Garcia et al., 2021; Lang et al., 2022; Wang et al., 2022; Xiao et al., 2022; Fan et al., 2023a; Guo et al., 2023; Dai et al., 2023a; Fan et al., 2016; Xu et al., 2024). Indeed, the iron sulfide phases formed in sulfidated ZVI particles promote electron transfer due to their good conductivity, enhancing dechlorination reactions (He et al., 2018; Xiao et al., 2022; Fan et al., 2017). Sulfur addition increases the hydrophobicity of the particles, which inhibits water reduction and H_2 evolution, thus directing electrons more effectively toward the dechlorination reaction (i.e., increasing selectivity) (He et al., 2018; Gong et al., 2020; Cai et al., 2021; Wu et al., 2023; Guo et al., 2023; Dai et al., 2023a). Also, with limited H_2 recombination, more H* is available for dechlorination reactions (Xiao et al., 2022). Finally, sulfides protect ZVI from passivation, potentially extending the treatment duration (Fan et al., 2023a).

Sulfidated ZVI-based materials have been widely investigated for their application in degrading chlorinated compounds in the aqueous phase, and recent publications suggest that it is still a topic of significant research interest (Dai et al., 2023b; Fan et al., 2023b; Gong et al., 2024; Qian et al., 2023; Sun et al., 2024; Xu et al., 2024; Yan et al., 2024). However, to our knowledge, no previous study has investigated the effectiveness of sulfidated materials for vapor phase remediation of chlorinated compounds. Therefore, this study aims to fill this gap by conducting experimental and modeling tests on chlorinated vapors to evaluate the feasibility of using sulfidated ZVI bimetals as passive reactive barriers in the unsaturated zone, specifically HPRBs, placed above contaminated soil or groundwater for the degradation of contaminated vapors. To this end, various ZVI-based materials were produced using different combinations of ZVI, sulfur (S), copper (Cu), and nickel (Ni), with molar ratios ranging from 0.05 to 0.2. Degradation batch tests were then carried out on both freshly produced and aged materials to assess their reactivity, kinetic degradation constants, and formed reaction byproducts, using TCE as a model compound. For the most reactive material, S-ZVI-Ni, TCE vapors diffusion column tests were also conducted to test the material at HPRB conditions for treating chlorinated vapors in the subsoil. Based on the results obtained, general guidelines for scaling up the proposed technique for field applications are provided.

2. Materials and methods

2.1. Materials and chemicals

The iron powder (ZVI), supplied by iPutec GmBH, was the same already used to produce bimetallic particles in previous studies performed by our group for TCE vapors dechlorination (Settimi et al., 2022, 2023). ZVI bimetals were synthesized using iron powder with copper (Cu) powder (purity ≥99 % and particle size lower than 75 μm) or nickel (Ni) powder (purity ≥99.7 % and particle size lower than 50 μm). Cu and Ni powders were both supplied by Sigma-Aldrich. Sulfidated ZVI and sulfidated bimetals were produced using also sulfur (S) powder supplied by Apollo Scientific.

These powders were put together in a disc mill (30 min, 700 rpm) at different combinations for producing the ZVI-based materials used in the TCE degradation tests and compared with ZVI (see Section S1 of the Supporting Information for further details on materials production). Namely, as summarized in Table S1 of the Supporting Information, starting from the mentioned powders, eight ZVI-based materials were synthesized: two bimetals (named ZVI-0.05Cu and ZVI-0.05Ni respectively) with Cu/ZVI or Ni/ZVI molar ratio of 0.05, two sulfidated ZVI samples, characterized by S/ZVI molar ratios of 0.05 and 0.2 (named respectively 0.05S-ZVI and 0.2S-ZVI), two sulfidated ZVI-Cu bimetals (named respectively 0.05S-ZVI-0.05Cu and 0.2S-ZVI-0.05Cu) and two sulfidated ZVI-Ni bimetals (named respectively 0.05S-ZVI-0.05Ni and 0.2S-ZVI-0.05Ni) with Cu/ZVI or Ni/ZVI molar ratio fixed at 0.05 and S/ZVI molar ratios of 0.05 and 0.2.

Sand with particles size between 0.5 and 2 mm was used for the column tests. TCE (purity ≥99.5 %) supplied by Honeywell was used for the degradation tests. 1,2-cis-dichloroethylene (1,2-cis-DCE) (purity ≥99.5 %) supplied by Sigma-Aldrich was used for the reaction byproducts estimation.

2.2. Characterization analyses

The produced ZVI-based materials were characterized using different techniques. The specific surface area (SSA) was evaluated using a gas sorption analyzer (Micromeritics TriStar II PLUS) and calculated according to Brunauer-Emmett-Teller (BET) method, using N_2 adsorption at 77 K (−196 °C). Before the analyses, the samples were pretreated under nitrogen flow for 2 h at 200 °C (Zingaretti et al., 2019). The investigation of bimetal formation and sulfidation occurrence was evaluated by X-ray diffraction (XRD) analyses using a Rigaku Diffractometer in the Bragg Brentano configuration (θ-2θ scans, range of 40–85°, Cu Kα radiation) (Settimi et al., 2022). The morphology and dimensions of the particles and the elemental mapping were evaluated using Scanning Electron Microscopy (SEM) equipped with an Energy-Dispersive X-ray Spectroscopy (EDS) (Nanoeye SNE-Alpha).

2.3. Aging of the materials

The aging of the materials was promoted to assess the effect of passivation on TCE dechlorination performances. Aging conditions were created by putting 3 ± 0.03 g of each material at the bottom of 4 mL transparent glass vials and adding 0.3 ± 0.03 mL of ultrapure (UP) water (Zeener Power II purification system) corresponding to 10 % by weight content on the material. After, the wet materials were left in contact with air (i.e., aerobic conditions) for 30 days at room temperature (22 ± 2 °C).

2.4. Degradation tests of TCE vapors

2.4.1. Batch tests

Batch degradation tests of TCE vapors were carried out at partially saturated conditions using a consolidated experimental set-up, already adopted in other studies performed by our group (Zingaretti et al., 2019,

2020; Settimi et al., 2022, 2023). Notably, degradation batch tests were conducted in sealed glass vials containing the reactive material with 10 % water by weight and a glass tube containing pure TCE, achieving an initial concentration in the vapor phase of 340 g m^{-3}. In parallel, vapor losses from the vials were assessed by performing control tests without the reactive material, allowing normalization of TCE concentration in the degradation tests (see Fig. S5 of the Supporting Information). Further details on this experimental procedure are reported in Section S3.1 of the Supporting Information.

A first set of batch tests was performed to observe the kinetic trends of the removal of TCE vapors induced by the produced materials at different reaction times in the range of 4 hours-4 days. The materials involved in TCE degradation tests were not subjected to pretreatments (e.g., acidic washing) after their synthesis, and the tests were performed under aerobic conditions.

Then, another set of batch tests was performed with the aged materials at a fixed time of 24 h to evaluate the reactivity of the materials towards dechlorination after the aging process, in which passivation could occur.

At the end of each test, the residual TCE and byproduct vapor concentrations were quantified by gas chromatography with a flame ionization detector (GC-FID). At the same time, the reaction byproducts were identified through gas chromatography with a mass spectrometer detector (GC-MS). For the GC-FID and GC-MS analyses, 250 μL of gas were taken by the syringe of the autosampler (PAL System, AOC-5000plus) from the headspace of the vials and injected (split ratio 1:10) in the GC (Shimadzu GC, GC_QP2010SE). The gas chromatograph was equipped with a Zebron ZB-5 (30 m × 0.25 mm ID × 0.25 μm film thickness), and a helium flow rate of 0.9 mL/min was applied for the analysis. The oven temperature started at 30 °C, held for 2 min, and increased at a rate of 8 °C/min to 150 °C, held for another 2 min. The TCE limit of quantification (LOQ) of the instrument was 0.01 g m^{-3}.

2.4.2. Column tests

Column degradation tests of TCE vapors were performed to observe the treatment performances of a reactive layer during time, thus simulating the treatment of vapors in an HPRB. The material used as a reactive layer in the column tests was the sulfidated ZVI-Ni bimetal with S/ZVI and Ni/ZVI molar ratios of 0.05. The experimental set-up adopted to perform column tests is reported in Fig. 1 and consists of a glass column provided with soil gas sampling ports (P1-P6). In order from the bottom, the column was filled with an 11 cm-glass beads layer with pure TCE (i.e., source), a 9 cm-level of sand, a 5 cm-reactive layer with 10 % of water content by weight, and a final 10 cm-glass beads layer. Further details on the column test layout are reported in Section S3.2 of the Supporting Information. The column tests were carried out in duplicate and maintained for 25 days. During the tests, vapors were collected from the sampling ports and analyzed using GC-FID and GC-MS with the settings already described in Section 2.4.1.

3. Results and discussion

3.1. Characterization of the materials

The reactive materials, i.e., ZVI, bimetals and sulfidated materials, showed relatively low specific surface area (0.03–2 m^2g^{-1}) quantified with the BET method. From XRD analyses, the formation of the bimetallic phases and the occurrence of sulfidation were observed (see Section S2.2 of the Supporting Information). Specifically, as already discussed in Settimi et al. (2022), the iron peak shift and the disappearance of the Ni or Cu characteristic peaks in the XRD analyses confirmed the bimetal formation through the incorporation of the secondary metals in the ZVI phase (see Figs. S1–S2 of the Supporting Information). Instead, sulfidation was confirmed by observing the formation of the FeS phase (see Fig. S2 of the Supporting Information). The shape and size of the particles of the sulfidated ZVI-based materials

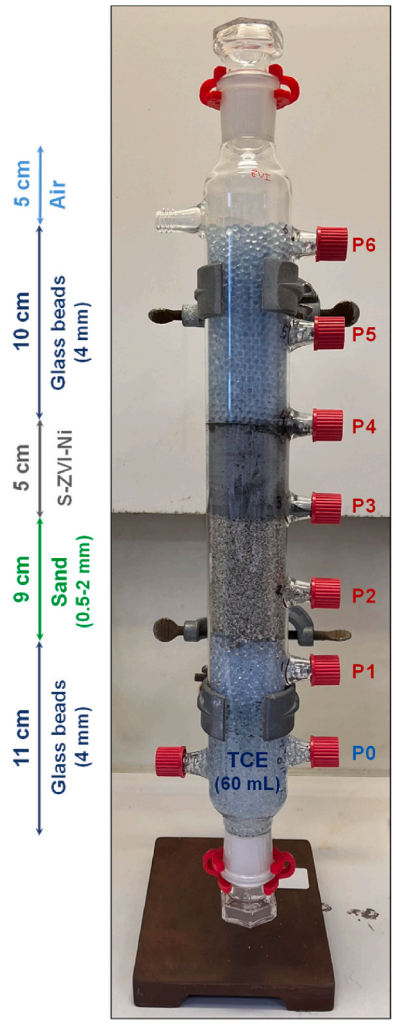

Fig. 1. Column degradation tests of TCE vapors layout using S-ZVI-Ni sulfidated bimetal.

produced were observed by SEM analyses (see Figs. S3–S4 of the Supporting Information). The particles of all the sulfidated materials were characterized by micrometric dimensions (in the range of 10–100 μm), with sulfidated ZVI samples (0.05S-ZVI and 0.2S-ZVI) showing overall smaller particles (in the range of 5–50 μm) compared to sulfidated bimetals. Increasing the sulfur dosage from 0.05 to 0.2 in the production of materials appears to increase the roughness on the surface of the particles, probably related to sulfides or sulfur presence in the free phase. Furthermore, EDS analyses were performed on the sulfidated materials to assess the distribution of S, Ni and Cu on the particles. As can be seen in Fig. 2, sulfur (blue dots) and secondary metals, i.e., Ni (yellow dots) or Cu (red dots), resulted in homogeneous distribution in the iron phase (green dots). Similar considerations were reported by Settimi et al. (2022) for non-sulfidated ZVI-Cu and ZVI-Ni bimetals since micrometric dimensions of the particles and homogeneous distribution of the secondary metals on iron were observed.

Further details on the characterization results are discussed in Section S2 of the Supporting Information.

3.2. Degradation of TCE vapors in batch tests using different ZVI-based materials

The results of the TCE degradation batch tests carried out using the produced materials are reported in Fig. 3 in terms of normalized concentrations of TCE in the vapor phase (C/C_{CTR}) as a function of time (t).

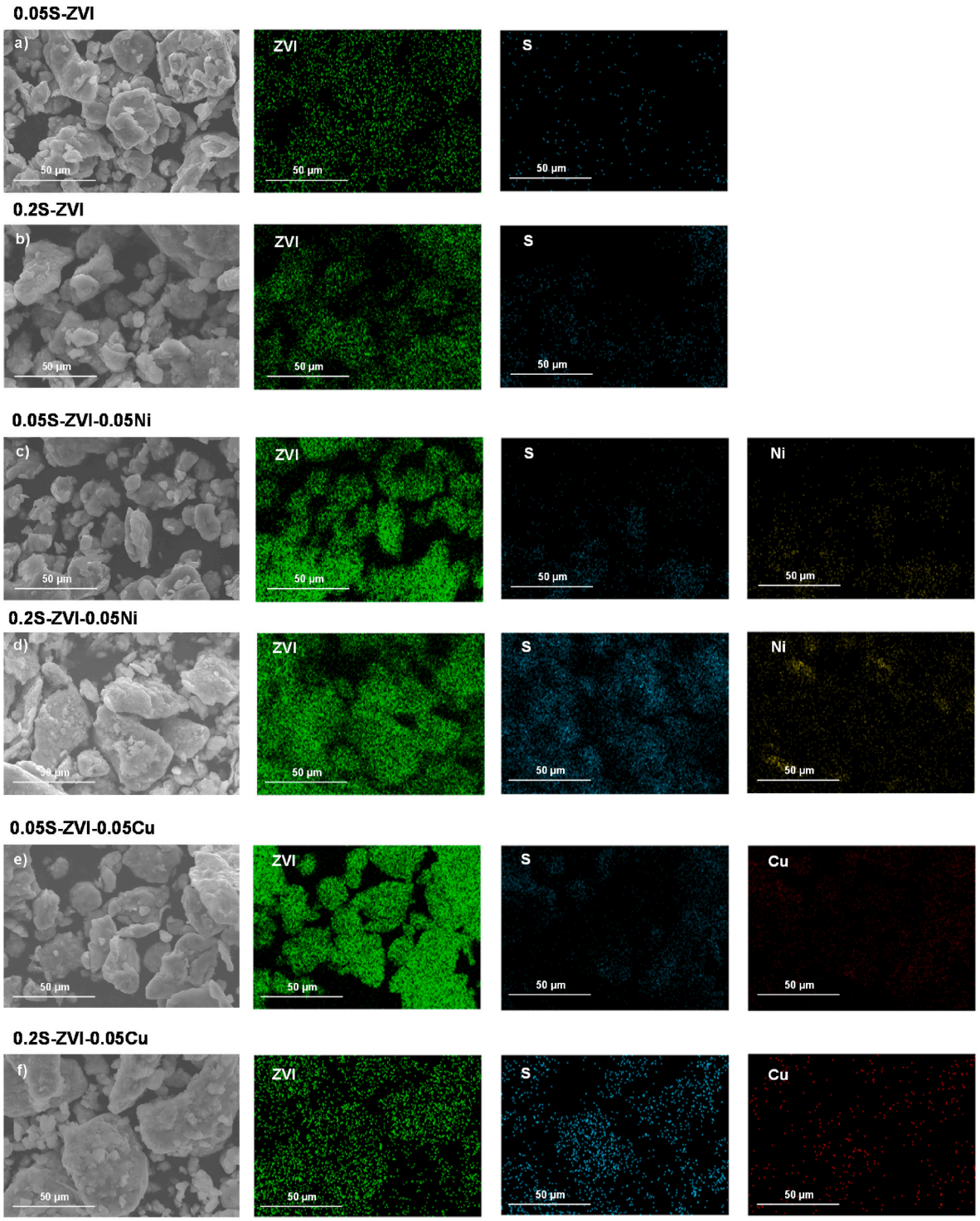

Fig. 2. SEM images and EDS maps for 0.05S-ZVI (a), 0.2S-ZVI (b), 0.05S-ZVI-0.05Ni (c), 0.2S-ZVI-0.05Ni (d), 0.05S-ZVI-0.05Cu (e), 0.2S-ZVI-0.05Cu (f).

For each tested material, a specific kinetic trend of TCE degradation (represented as dashed or continuous lines in Fig. 3) was determined on the basis of the experimental data (represented as points in Fig. 3). In particular, zero-order (i.e., linear) and first-order (i.e., exponential) degradation kinetics were derived with the relationships reported in Equation (1) and Equation (2), respectively (Zingaretti et al., 2020; Settimi et al., 2023):

$$\frac{C}{C_{CTR}} = -\frac{k_0}{C_0}t + 1 \qquad \text{Equation 1}$$

$$\frac{C}{C_{CTR}} = e^{-k_1 t} \qquad \text{Equation 2}$$

Where C (g m^{-3}) and C_{CTR} (g m^{-3}) are the residual TCE concentrations in vapors detected at the end of each degradation and control test, respectively. In the zero-order degradation kinetic equation, k_0 (g m^{-3}d^{-1}) refers to the zero-order degradation constant and C_0 (g m^{-3}) is the initial TCE concentration used in the tests (i.e., 340 g m^{-3}). Instead, in the equation describing the first-order degradation kinetics, k_1 (d^{-1}) is the first-order kinetic constant. t (d) is the reaction time ranging from

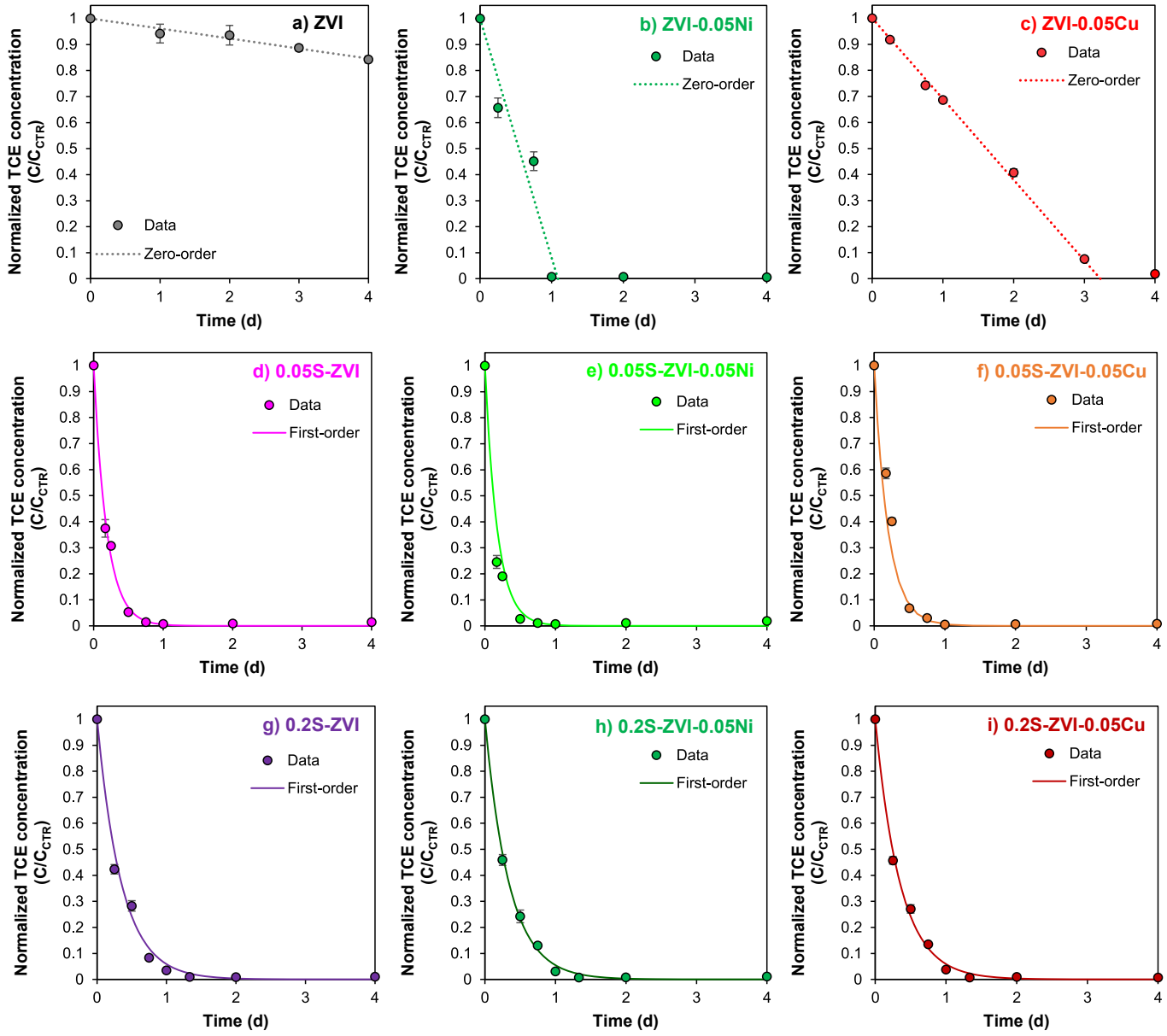

Fig. 3. Experimental data relative to the degradation of TCE vapors (point) using ZVI-based materials. The error bars indicated the standard deviation of the tests conducted in duplicate. Zero-order (dashed line) and first-order (continuous line) kinetic trends are also reported. The kinetic trends were fitted for data until 24 h (b, d-f), 3 d (c), 2 d (g–i).

4 h to 4 d in the tests. The kinetic trends and constants observed in the experiments using the tested materials are reported in Table 1.

Using ZVI alone, a degradation of TCE of only 15 % was achieved in 4 days (Fig. 3a). Adding the secondary metal (i.e., Cu or Ni) to ZVI, improved TCE degradation performance (see Fig. 3b and c). Specifically, using ZVI-0.05Cu bimetal (Figs. 3b), 98 % of TCE removal was achieved in 4 days, while using ZVI-0.05Ni (Figs. 3c), 99 % of TCE removal was observed in 24 h. In line with previous studies on aqueous and vapor phases, Ni proved to be a better catalyst for ZVI-induced dechlorination than Cu (Kim and Carraway, 2003; Venkateshaiah et al., 2022; Settimi et al., 2023). It is indeed recognized that Cu enhances electron transfer through iron particles, thereby improving the dechlorination reaction (Kim and Carraway, 2003; Settimi et al., 2022). Conversely, Ni also catalyzes the dissociation of molecular hydrogen, increasing the availability of electrons and atomic hydrogen needed for dechlorination reactions (Kim and Carraway, 2003; Settimi et al., 2022). In the tests with bimetals, the experimental data followed a zero-order kinetic with estimated degradation constants of 105 and 312 g $m^{-3}d^{-1}$ for ZVI-0.05Cu and ZVI-0.05Ni, respectively. These results are comparable to our previous study, in which similar bimetals were used to degrade

Table 1
Kinetic degradation constants (k_0 and k_1) evaluated for the tested materials.

Material	Kinetic order	k_1 (d^{-1})	k_0 (g $m^{-3}d^{-1}$)	R^2 (–)
ZVI	zero-order	–	13.09	0.96
ZVI-0.05Ni	zero-order	–	312.8	0.93
ZVI-0.05Cu	zero-order	–	105.4	0.98
0.05S-ZVI	first-order	5.29	–	0.99
0.05S-ZVI-0.05Ni	first-order	5.66	–	0.98
0.05S-ZVI-0.05Cu	first-order	5.06	–	0.96
0.2S-ZVI	first-order	2.84	–	0.99
0.2S-ZVI-0.05Ni	first-order	2.91	–	0.99
0.2S-ZVI-0.05Cu	first-order	2.83	–	0.99

TCE vapors (Settimi et al., 2023).

Although the addition of a secondary metal to ZVI led to an increase in TCE dechlorination compared to using only ZVI, a further improvement was observed when sulfidation was performed on iron and bimetals. Differently from bimetals, TCE degradation followed a first-order kinetic when sulfur was added to the materials, in line with previous studies on TCE degradation in the aqueous phase using S-ZVI (Han and Yan, 2016; Cai et al., 2021; Lang et al., 2022) and sulfidated bimetals (Fan et al., 2023b). Specifically, adding sulfur to ZVI at a molar ratio of 0.05 (i.e., 0.05S-ZVI material in Fig. 3d) led to up to 99 % removal of TCE vapors in 18 h, with a first-order degradation constant of 5.3 d^{-1}. The TCE degradation achieved with 0.05S-ZVI was higher than that obtained using ZVI-0.05Cu and ZVI-0.05Ni bimetals, aligning with the results observed in previous literature for the degradation in the aqueous phase. For instance, He et al. (2018) tested S-ZVI, ZVI-Cu, and ZVI-Ni for degrading TCE in the aqueous phase and observed better performances using S-ZVI compared to bimetals. Similarly, Yang et al. (2023) observed better performances with milled S-ZVI compared to ZVI-Cu for Chromium(VI) degradation.

The further addition of Ni or Cu to sulfidated iron entailed similar degradation with slightly different effects. In the case of 0.05S-ZVI-0.05Ni (see Fig. 3e), up to 99 % of TCE removal was achieved in 18 h with a slightly higher degradation kinetic constant of 5.7 d^{-1}. As a reference, Tian et al. (2022) combined Ni and S with ZVI, finding higher atrazine degradation in water using sulfidated ZVI-Ni bimetal than sulfidated iron. Conversely, a slightly slower degradation rate was observed with 0.05S-ZVI-0.05Cu, reaching up to 99 % of TCE removal in 24 h with a first-order degradation constant of 5 d^{-1} (0.05S-ZVI-0.05Cu in Fig. 3f). Increasing the S content in the produced materials, i.e., adopting a S/ZVI molar ratio of 0.2 instead of 0.05, decreased the performances of TCE dechlorination. Namely, 0.2S-ZVI led to 99 % of TCE removal in 32 h, with a first-order degradation constant of 2.8 d^{-1} (Fig. 3g). Similar results were obtained with 0.2S-ZVI-0.05Ni and 0.2S-ZVI-0.05Cu, for which up to 99 % of TCE removal was observed in 32 h with first-order degradation constant values of 2.9 and 2.8 d^{-1}, respectively (Fig. 3h–i). These findings align with some studies conducted in the aqueous phase (e.g., Lang et al., 2022; Mangayayam et al., 2019; Mo et al., 2022; Xu et al., 2020), which observed decreased TCE dechlorination by increasing S loading in the particles. In fact, increasing the S content in the sulfidation process could decrease dechlorination due to a higher presence of FeS on the ZVI particles that block active sites for H* adsorption (Mangayayam et al., 2019; Mo et al., 2022).

As shown in Table S2 of the Supporting Information, all the tested materials were characterized by low specific surface area (SSA) values in the range of 0.03–2 m^2g^{-1}. These results suggest that the improved TCE removal observed compared to ZVI alone is mainly driven by catalyzed electron transfer and atomic hydrogen availability from the addition of Cu, Ni, or S.

3.3. Byproducts and degradation pathway

For evaluating the formation of byproducts and the TCE degradation pathway, GC-MS was used to identify the byproducts detectable at each reaction time, whereas GC-FID was adopted for quantifying the concentrations. Further details about the byproducts detected at different reaction times are reported in Section S4 of the Supporting Information.

Generally, C_3-C_6 hydrocarbons were the main reaction byproducts observed under all tested conditions (see Figs. S7–S9 for the detailed compounds identified by GC-MS). Using ZVI and ZVI-Ni bimetal, dichloroacetylene (C_2Cl_2), 1,1-dichloroethylene (1,1-DCE) and 1,2-cis-dichloroetylene (1,2-cis-DCE) and vinyl chloride (VC) were also detected as degradation byproducts (see Table S3 of the Supporting Information), although to a lower extent (see Fig. S6 of the Supporting Information). Using ZVI-Cu bimetal, all the mentioned compounds were detected over time, excluding VC (see Table S3 of the Supporting Information). Instead, using sulfidated materials, dichloroacetylene was not detected (see Table S3 of the Supporting Information). DCE (both 1,1-DCE and 1,2-cis-DCE) and VC are typical byproducts of TCE reductive dehalogenation through hydrogenolysis pathway, while dichloroacetylene and C_3-C_6 hydrocarbons are typical of the β-elimination pathway of chlorinated ethenes (Campbell et al., 1997; Liu et al., 2005). It is worth noting that no C_2 compounds typically associated with the β-elimination pathway, such as ethylene, chloroacetylene or acetylene (Arnold and Roberts, 2000; Campbell et al., 1997; Liu et al., 2005; Zhang et al., 2021), were detected in the tested conditions. The non-detection of chloroacetylene or acetylene can likely be attributed to the high reactivity of these byproducts as transient intermediates in zero-valent metal systems, where they undergo rapid reduction upon contact with metal surfaces in the gas phase (Arnold and Roberts, 2000; Campbell et al., 1997; Zingaretti et al., 2019). However, considering the detected byproducts, it can be concluded that both hydrogenolysis and β-elimination mechanisms were active, although the latter was predominant due to the high presence of C_3-C_6 hydrocarbons (see Fig. S6 of the Supporting Information and Fig. 5).

Based on the detected byproducts in each system tested, Fig. 4 shows the two dechlorination pathways assumed for the degradation of TCE in the vapor phase. TCE was reduced to DCE (1,2-cis-DCE and 1,1-DCE) and consequently to VC by hydrogenolysis pathway. At the same time, the transformation to dichloroacetylene (using ZVI and bimetals) or directly chloroacetylene (using sulfidated materials) occurred until reaching the formation of C_3-C_6 hydrocarbons. It is worth noting that chloroacetylene is usually recognized as the first intermediate of TCE through β-elimination pathway (Campbell et al., 1997; Liu et al., 2005). However, since dichloroacetylene was detected in some cases in this study, though at low levels (see Fig. S6 of the Supporting Information), the transformation of TCE in this intermediate was also proposed (Fig. 4).

TCE is recognized as a carcinogenic compound (IARC, 2014). Among the detected byproducts of TCE degradation, VC is the most critical since it is considered carcinogenic and has more critical toxicological properties than the initial TCE (IARC, 2014). However, VC was formed to a lower extent by a minor hydrogenolysis pathway, while most of the byproducts were in the majority C_3-C_6 hydrocarbons from β-elimination. The detected C_3-C_6 were mostly non-carcinogenic compounds, according to the IARC classification.

Fig. 4 also shows the proposed mechanism of TCE degradation, in which the presence of ZVI induces TCE dechlorination by electron release (Arnold and Roberts, 2000). The addition of Cu or Ni to ZVI enhances the electron transfer through the particles, increasing TCE degradation (He et al., 2018; Kim and Carraway, 2003). Additionally, Ni increases the availability of H* from H_2 dissociation, for which Ni is a catalyst (Kim and Carraway, 2003). Finally, adding S further enhances electron transfer due to the presence of FeS and limits the formation of iron oxides (Fe_xO_y) on the particle surface (Fan et al., 2017; Garcia et al., 2021).

The byproducts detected at each reaction time in the degradation tests were quantified to perform a TCE mass balance for all the tested materials (Fig. 5). Namely, the amount of residual TCE and byproducts measured at the end of each test was compared with the TCE mass measured in the corresponding control tests. The detailed mass balance calculations are provided in Section S5 of the Supporting Information. As shown in Fig. 5, the TCE mass balance accounted for over 70 % in each tested condition and almost 100 % in several cases. The discrepancy where the mass balance only reaches 70–80 % could be due to the assumptions made in the calculations of the response factors or the failure to quantify some expected byproducts of the two considered pathways (e.g., chloroacetylene, acetylene or ethylene). However, the mass balance results indicate that dechlorination was the leading cause of TCE removal in the vapor phase, and other effects, such as adsorption on the reactive material, could be considered negligible.

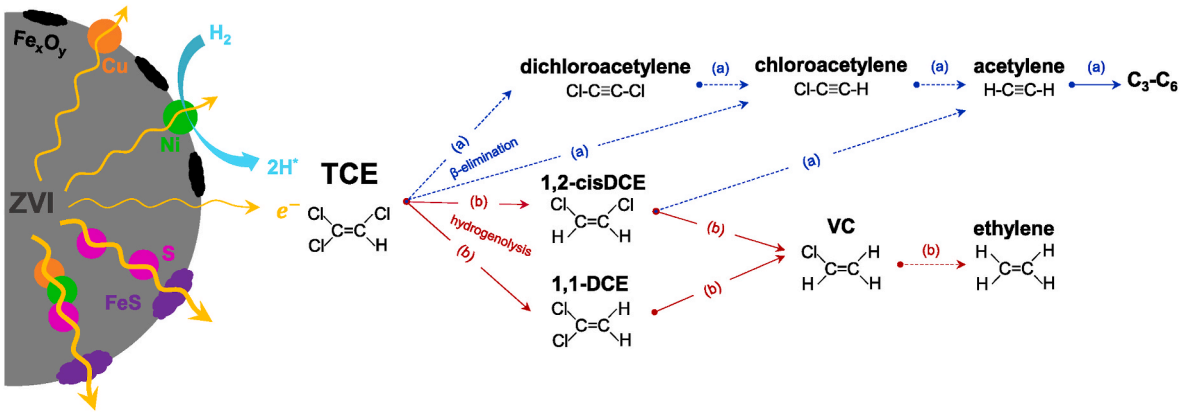

Fig. 4. Dechlorination mechanism and pathway of TCE (dotted lines if assumed) by ZVI-based materials.

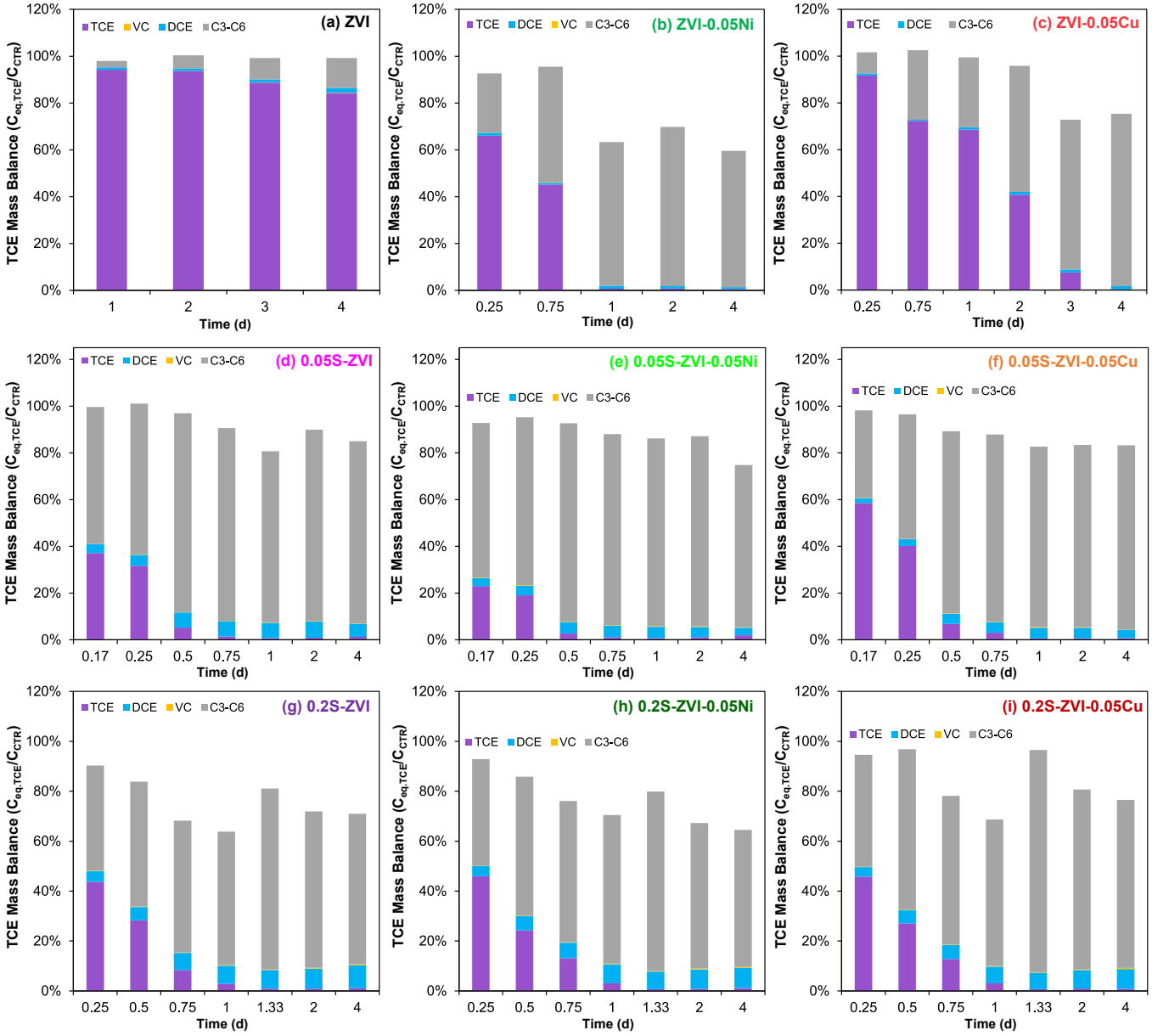

Fig. 5. TCE mass balance resulted from batch tests performed with ZVI-based materials (only detected byproducts by GC-FID are reported). DCE refers to the sum of 1,2-cis-DCE and 1,1-DCE.

3.4. Degradation of TCE after materials aging

Fig. 6 presents the results obtained in the batch degradation tests using different aged materials (exposed to air for 30 days) at 24 h of reaction. These results are compared with those observed using pristine ones. The materials tested included ZVI, ZVI-Cu, ZVI-Ni, 0.05S-ZVI, 0.05S-ZVI-0.05Cu and 0.05S-ZVI-0.05Ni. Sulfidated materials with a S/ZVI molar ratio of 0.2 were not considered in these tests, as they proved less reactive (see Section 3.2). From the results reported in Fig. 6, ZVI showed decreased efficacy, which was already low for the pristine material. Moreover, ZVI-Ni and ZVI-Cu lost their efficacy towards dechlorination after aging, probably due to passivation phenomena. As a reference, Grenier et al. (2004) tested ZVI and ZVI-Ni particles for 1, 2-cis-DCE vapors dechlorination in column aerobic experiments, observing a loss of efficacy due to the formation of oxide layers after 7 days of reaction. Similarly, Qu et al. (2021) observed a loss in the degradation ability of Chromium(VI) by using ZVI and ZVI-Cu after aging the materials by exposure to air.

Conversely, sulfidated materials remained reactive after aging, maintaining more than 99 % TCE removal, i.e., comparable to the freshly produced material. These results highlight the importance of sulfidation in preserving the longevity of the treatment by preventing passivation. These results align with previous literature regarding the degradation of chlorinated compounds in water using sulfidated ZVI (Gu et al., 2019; Mangayayam et al., 2019; Xu et al., 2019; Fan et al., 2023a; Han and Yan, 2016). The anti-passivation effect in sulfidated materials is due to the presence of FeS phases that protect the ZVI particles from oxide formation, maintaining efficient electron transfer through ZVI (Gu et al., 2019; Fan et al., 2023a). For example, Mangayayam et al. (2019) found S-ZVI particles still reactive toward TCE dechlorination in water after 30 days of aging.

Thus, for using these materials to fill HPRBs placed in the unsaturated zone, sulfidation is necessary to maintain the degradation efficiency of chlorinated vapors in the field, where air and humidity are present. It is worth noting that, in this work, simplified aging conditions were performed on the materials by exposure to only air and humidity. However, other factors including the presence of multiple oxidizers or microbial activity in the subsurface should be considered to address more realistic aging conditions.

3.5. Degradation of TCE vapors in column using S-ZVI-Ni

The column was filled with a reactive layer of S-ZVI-Ni (0.05S-ZVI-0.05Ni), which showed the highest dechlorination rate among the tested materials (see Fig. 3) and resistance to passivation (see Fig. 6). The milling conditions for producing the reactive material used in the column test were slightly adjusted compared to those adopted for the batch tests. These adjustments included changes in the quantity of powder used in the mill and the milling speed. For more details, refer to Section S6 of the Supporting Information.

The column tests were performed under diffusive flow conditions since diffusion is considered the dominant transport for vapors in the unsaturated zone (Conant et al., 1996; Verginelli and Yao, 2021; Yao et al., 2013; You and Zhan, 2013).

Fig. 7 shows the normalized TCE vapors concentration profiles detected in the columns as a function of the vertical distance from the first soil gas sampling port of the column (P1) used as a reference. The concentrations of TCE detected in the different sampling ports were normalized to the ones detected at the sampling port P1 (see Fig. 1). Considering the column set-up, it was estimated that TCE vapors in the column are expected to reach the reactive layer in 2 h, exit the layer in 28 h, and then reach the top of the column (i.e., port P6) in 30 h (see Section S8 of the Supporting Information for the diffusion time estimations). TCE vapors sampling from the column and subsequent analyses were performed at 1, 4, 7, 10, 15 and 25 days. From Fig. 7, after 4 days of diffusion (i.e., after the expected diffusion time of vapors through the reactive layer), TCE concentrations decreased in the reactive layer (i.e., from port P3 to P4), achieving an average TCE removal of 68 %. The TCE abatement remained quite constant throughout the test duration, with trichloroethylene removal ranging from 66 % to 80 % after analyzing samples from the column after 7–25 days. The sustained TCE removal over time indicated that passivation did not influence the material reactivity and, consequently, the treatment efficiency in column tests, likely due to sulfidation.

The same reaction byproducts already detected in the batch tests using S-ZVI-Ni were found during the column test, namely C_3-C_6 hydrocarbons and, to a lower extent, DCE (1,1-DCE and 1,2-cis-DCE) and VC. A TCE mass balance was performed over time, considering the concentrations detected entering and exiting the S-ZVI-Ni reactive layer

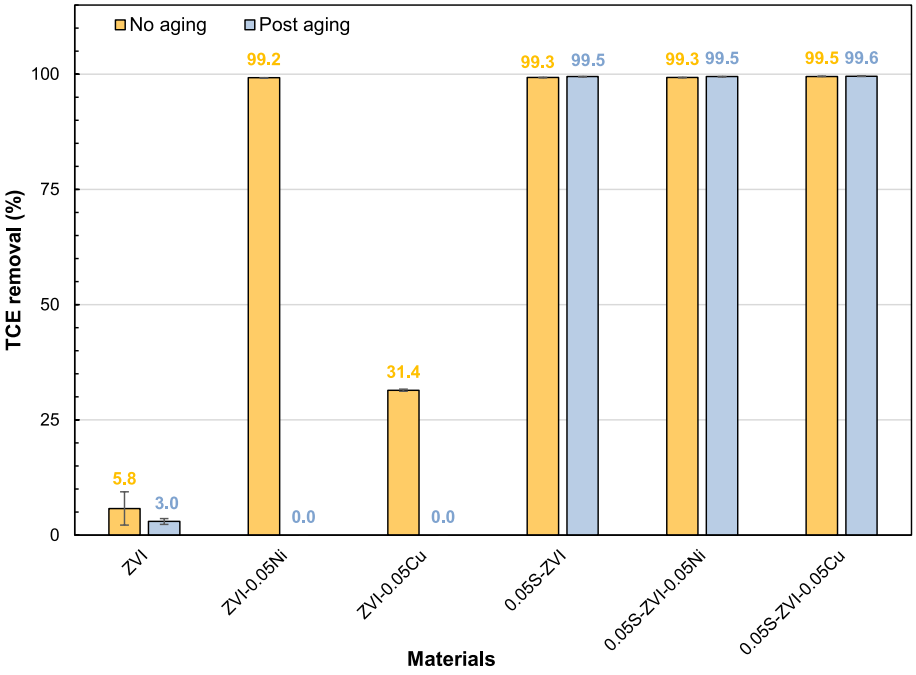

Fig. 6. Degradation of TCE in batch tests at 24 h with aged materials compared with no aged ones.

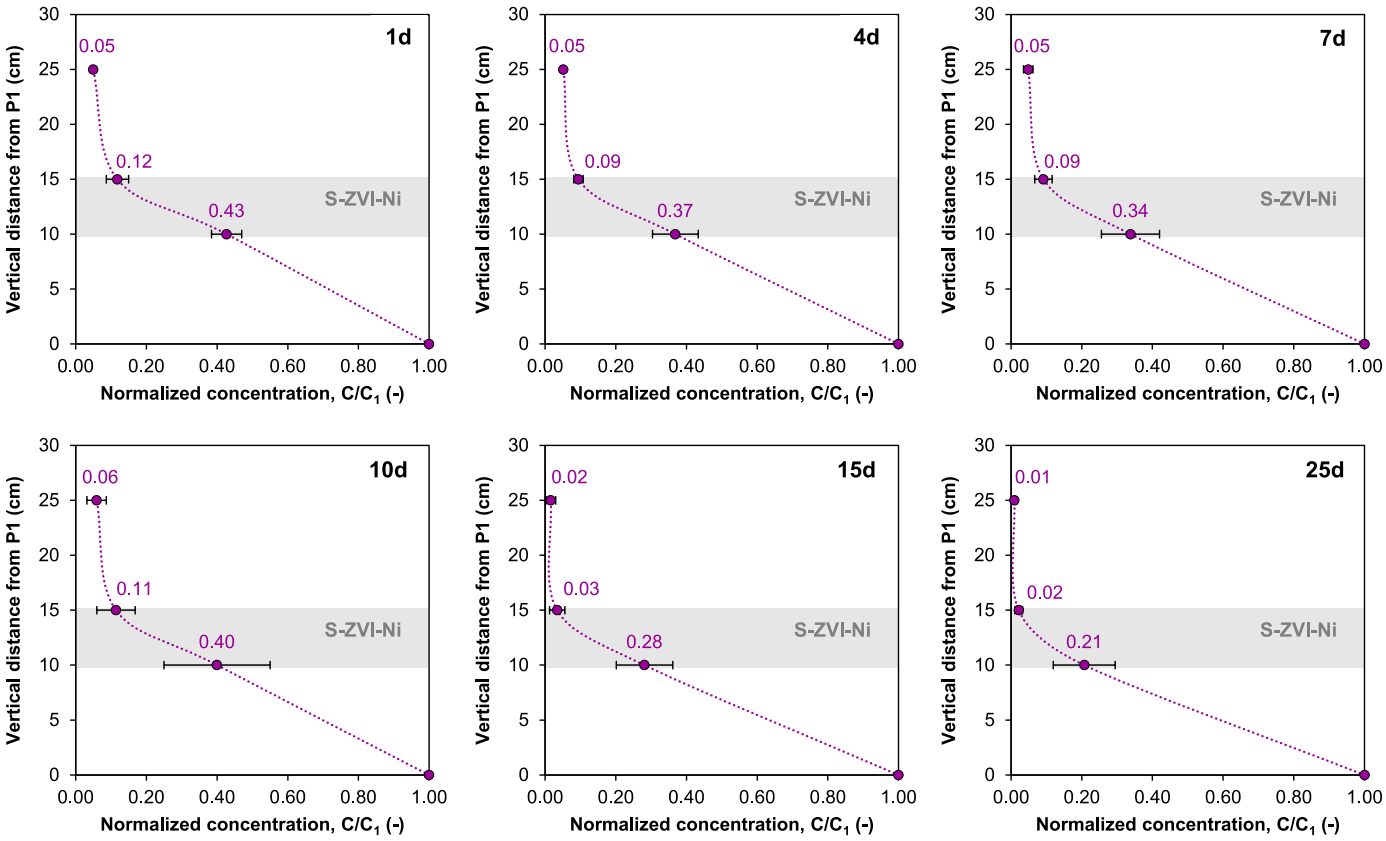

Fig. 7. Normalized TCE concentration profiles in column tests using S-ZVI-Ni in time. The reactive layer is between 10 and 15 cm (grey rectangle). The error bars indicate the deviation standard of the replicates.

(see Section S5 and Fig. S10 of the Supporting Information). As in the batch tests, C_3-C_6 were the prevalent byproducts formed during reactions, followed by DCE and VC, both detected at lower concentrations. Both TCE and byproduct concentrations remained approximately constant during the test, thus maintaining the treatment efficacy over time. As observed in the batch tests, TCE degradation followed prevalent β-elimination and minor hydrogenolysis pathways from the detected byproducts.

3.6. Estimation of the thickness of the reactive barrier

Considering the potential use of the tested materials as passive barriers in the unsaturated zone for treating vapors emitted from contaminated soil or groundwater, it is possible to determine the necessary thickness of the reactive barrier to achieve the desired attenuation based on the results obtained. To this aim, the following analytical solution derived from a 1-D transport equation based on diffusion-dominated transport in a homogeneous soil can be used (Verginelli et al., 2017):

$$\frac{C_{out}}{C_{in}} = \exp\left(-\frac{\Delta z}{L_R}\right) \quad \text{Equation 3}$$

where C_{out} (g m^{-3}) and C_{in} (g m^{-3}) are the concentrations of the contaminant in the vapor phase outgoing and entering a reactive layer with a thickness of Δz (m) and L_R (m) is the diffusive reaction length.

As shown in Section S9 of the Supporting Information, using the above equation, the diffusion-reaction length obtained in both batch and column tests was in the range of 1–4 cm (see Fig. S13). Furthermore, by rearranging this equation, it is possible to calculate the minimum thickness of the reactive barrier, d_{HPRB} (m), needed to achieve the desired attenuation (Verginelli et al., 2017):

$$d_{HPRB} = -L_R \cdot \ln\left(\frac{C_{out,target}}{C_{in}}\right) \quad \text{Equation 4}$$

where $C_{out,target}$ (g m^{-3}) is the desired target concentration of the contaminant outgoing the barrier.

For example, considering a target attenuation of the concentrations in the vapor phase of 99 % (i.e., $C_{out,target}/C_{in} = 0.01$) and assuming the diffusive reaction length of 3.8 cm estimated in the column test (see Section S9 in the Supporting Information), the minimum thickness to achieve the mentioned removal is around 18 cm. This thickness is comparable to the ones previously estimated by Settimi et al. (2023) for bimetals (12–18 cm) and significantly lower than that estimated by Zingaretti et al. (2020) for iron alone (100 cm) from batch degradation tests of TCE vapors. This result further highlights the suitability of the tested sulfidated bimetal for passive vapor treatment in the unsaturated zone. It is worth noting that a diffusion-dominated transport of vapors and homogeneous soil conditions were considered to derive the analytical solution for the HPRB thickness estimation. As previously reported, diffusion is considered the main transport mechanism for the transport of vapors in the unsaturated zone (Verginelli and Yao, 2021; You and Zhan, 2013). However, advective transport (e.g., due to water table fluctuations, barometric pumping or temperature gradients) (Massmann and Farrier, 1992; McHugh and McAlary, 2009) and non-homogeneous soil conditions (Bozkurt et al., 2009) can affect vapors transport. Therefore, the estimates provided in this section should be considered as a preliminary screening. However, for the design of barrier thickness and configuration, the use of more advanced numerical models may be more appropriate.

4. Conclusions

The obtained results showed that sulfidated ZVI-based materials can be an effective and durable option for the treatment of chlorinated solvents in the vapor phase. Such materials could be suitable for filling HPRBs in the unsaturated zone to promote passive remediation of chlorinated vapors and manage the related risks in a more sustainable way compared to traditional techniques. Sulfidated materials showed high reactivity towards the dechlorination of TCE vapors in the degradation batch tests performed. Furthermore, the obtained results showed that, compared to ZVI and bimetals, sulfidated materials ensure the maintenance of the treatment efficiency over time under conditions partially resembling those expected in the field, simulated through the exposure of reactive materials to air and humidity. Therefore, sulfidation demonstrates an effective modification technique for ZVI-based materials to enhance reactivity towards dechlorination and contrast passivation, thus increasing the durability of the treatment. Using sulfidated materials, TCE degradation primarily followed the β-elimination pathway, forming C_3-C_6 hydrocarbons as reaction byproducts. Lower amounts of DCE and VC were also detected as intermediates, indicating that hydrogenolysis was a secondary degradation pathway and the formation of carcinogenic byproducts like VC was limited. By integrating the results of the column tests into a simple analytical model, it was found that a low thick reactive layer of 18 cm based on sulfidated ZVI-Ni bimetal could ensure up to 99 % degradation of TCE vapors. Therefore, the overall results indicate that sulfidated ZVI-based materials have the potential for their use as filling materials for HPRBs, thus representing an efficient and durable solution for passive remediation of chlorinated vapors at contaminated sites.

CRediT authorship contribution statement

Clarissa Settimi: Writing – original draft, Methodology, Investigation, Formal analysis, Data curation, Conceptualization. **Daniela Zingaretti:** Writing – review & editing, Supervision, Methodology, Conceptualization. **Iason Verginelli:** Writing – review & editing, Supervision, Methodology, Conceptualization. **Renato Baciocchi:** Writing – review & editing, Resources, Project administration, Funding acquisition.

Declaration of competing interest

The authors declare that they have no known competing financial interests or personal relationships that could have appeared to influence the work reported in this paper.

Acknowledgments

The authors would like to thank Cadia d'Ottavi and Leonardo Duranti from the Department of Chemical Science and Technologies of the University of Rome Tor Vergata for the BET analyses, Simone Sanna and Antonello Tebano from the Department of Civil Engineering and Computer Science Engineering of the University of Rome Tor Vergata for the XRD analyses, and Gabriele Baiocco from the Department of Industrial Engineering of the University of Rome Tor Vergata for the SEM-EDS analyses.

Appendix A. Supplementary data

Supplementary data to this article can be found online at https://doi.org/10.1016/j.envpol.2025.126202.

Data availability

Data will be made available on request.

References

Arnold, W.A., Roberts, A.L., 2000. Pathways and kinetics of chlorinated ethylene and chlorinated acetylene reaction with Fe(0) particles. Environ. Sci. Technol. 34, 1794–1805. https://doi.org/10.1021/es990884q.

Bozkurt, O., Pennell, K.G., Suuberg, E.M., 2009. Simulation of the vapor intrusion process for nonhomogeneous soils using a three-dimensional numerical model. Groundw. Monit. Remediat. 29, 92–104. https://doi.org/10.1111/j.1745-6592.2008.01218.x.

Cai, S., Chen, B., Qiu, X., Li, J., Tratnyek, P.G., He, F., 2021. Sulfidation of zero-valent iron by direct reaction with elemental sulfur in water: efficiencies, mechanism, and dechlorination of trichloroethylene. Environ. Sci. Technol. 55, 645–654. https://doi.org/10.1021/acs.est.0c05397.

Campbell, T.J., Burris, D.R., Roberts, A.L., Wells, J.R., 1997. Trichloroethylene and tetrachloroethylene reduction in a metallic iron–water-vapor batch system. Environ. Toxicol. Chem. 16, 625–630. https://doi.org/10.1002/etc.5620160404.

Conant, B.H., Gillham, R.W., Mendoza, C.A., 1996. Vapor transport of trichloroethylene in the unsaturated zone: field and numerical modeling investigations. Water Resour. Res. 32, 9–22. https://doi.org/10.1029/95WR02965.

Dai, Y., Dong, Y., Duan, L., Zhang, B., Wang, S., Zhao, S., 2023a. Unraveling the neglected role of elemental sulfur in chromate removal by sulfidated microscale zero-valent iron. J. Hazard Mater. 449, 131025. https://doi.org/10.1016/j.jhazmat.2023.131025.

Dai, Y., Du, W., Jiang, C., Wu, W., Dong, Y., Duan, L., Sun, S., Zhang, B., Zhao, S., 2023b. Enhanced reductive degradation of chloramphenicol by sulfidated microscale zero-valent iron: sulfur-induced mechanism, competitive kinetics, and new transformation pathway. Water Res. 233, 119743. https://doi.org/10.1016/j.watres.2023.119743.

Fan, B., Li, X., Zhu, F., Wang, J., Gong, Z., Shao, S., Wang, X., Zhu, C., Zhou, D., Gao, S., 2023a. Anti-passivation ability of sulfidated microscale zero valent iron and its application for 1,1,2,2-tetrachloroethane degradation. J. Hazard Mater. 443, 130194. https://doi.org/10.1016/j.jhazmat.2022.130194.

Fan, B., Zhou, B., Chen, S., Zhu, F., Chen, B., Gong, Z., Wang, X., Zhu, C., Zhou, D., He, F., Gao, S., 2023b. Preparation of Fe/Cu bimetals by ball milling iron powder and copper sulfate for trichloroethylene degradation: combined effect of FeS and Fe/Cu alloy. J. Hazard Mater. 460, 132402. https://doi.org/10.1016/j.jhazmat.2023.132402.

Fan, D., Lan, Y., Tratnyek, P.G., Johnson, R.L., Filip, J., O'Carroll, D.M., Nunez Garcia, A., Agrawal, A., 2017. Sulfidation of iron-based materials: a review of processes and implications for water treatment and remediation. Environ. Sci. Technol. 51, 13070–13085. https://doi.org/10.1021/acs.est.7b04177.

Fan, D., O'Brien Johnson, G., Tratnyek, P.G., Johnson, R.L., 2016. Sulfidation of nano zerovalent iron (nZVI) for improved selectivity during in-situ chemical reduction (ISCR). Environ. Sci. Technol. 50, 9558–9565. https://doi.org/10.1021/acs.est.6b02170.

Fu, F., Dionysiou, D.D., Liu, H., 2014. The use of zero-valent iron for groundwater remediation and wastewater treatment: a review. J. Hazard Mater. 267, 194–205. https://doi.org/10.1016/j.jhazmat.2013.12.062.

Garcia, A.N., Zhang, Y., Ghoshal, S., He, F., O'Carroll, D.M., 2021. Recent advances in sulfidated zerovalent iron for contaminant transformation. Environ. Sci. Technol. 55, 8464–8483. https://doi.org/10.1021/acs.est.1c01251.

Gong, L., Chen, J., Shen, L., Zhang, Z., Xia, C., Wu, F., Yao, Y., Liu, C., Liang, L., He, F., 2024. Unveiling the mechanistic role of surface nitrogen and sulfur in boosting the dechlorination performance of zero-valent iron. ACS EST Eng. 4, 2284–2293. https://doi.org/10.1021/acsestengg.4c00241.

Gong, L., Lv, N., Qi, J., Qiu, X., Gu, Y., He, F., 2020. Effects of non-reducible dissolved solutes on reductive dechlorination of trichloroethylene by ball milled zero valent irons. J. Hazard Mater. 396, 122620. https://doi.org/10.1016/j.jhazmat.2020.122620.

Grenier, A.C., Mcguire, M.M., Fairbrother, D.H., Roberts, A.L., 2004. Treatment of vapor-phase organohalides with zero-valent iron and Ni/Fe reductants. Environ. Eng. Sci. 21, 421–435. https://doi.org/10.1089/1092875041358548.

Gu, Y., Gong, L., Qi, J., Cai, S., Tu, W., He, F., 2019. Sulfidation mitigates the passivation of zero valent iron at alkaline pHs: experimental evidences and mechanism. Water Res. 159, 233–241. https://doi.org/10.1016/j.watres.2019.04.061.

Gu, Y., Wang, B., He, F., Bradley, M.J., Tratnyek, P.G., 2017. Mechanochemically sulfidated microscale zero valent iron: pathways, kinetics, mechanism, and efficiency of trichloroethylene dechlorination. Environ. Sci. Technol. 51, 12653–12662. https://doi.org/10.1021/acs.est.7b03604.

Guan, X., Sun, Y., Qin, H., Li, J., Lo, I.M.C., He, D., Dong, H., 2015. The limitations of applying zero-valent iron technology in contaminants sequestration and the corresponding countermeasures: the development in zero-valent iron technology in the last two decades (1994–2014). Water Res. 75, 224–248. https://doi.org/10.1016/j.watres.2015.02.034.

Guo, J., Gao, F., Zhang, C., Ahmad, S., Tang, J., 2023. Sulfidation of zero-valent iron for enhanced reduction of chlorinated contaminants: a review on the reactivity, selectivity, and interference resistance. Chem. Eng. J. 477, 147049. https://doi.org/10.1016/j.cej.2023.147049.

Han, Y., Yan, W., 2016. Reductive dechlorination of trichloroethene by zero-valent iron nanoparticles: reactivity enhancement through sulfidation treatment. Environ. Sci. Technol. 50, 12992–13001. https://doi.org/10.1021/acs.est.6b03997.

He, F., Li, Z., Shi, S., Xu, W., Sheng, H., Gu, Y., Jiang, Y., Xi, B., 2018. Dechlorination of excess trichloroethene by bimetallic and sulfidated nanoscale zero-valent iron. Environ. Sci. Technol. 52, 8627–8637. https://doi.org/10.1021/acs.est.8b01735.

IARC, 2014. IARC Monographs on the Evaluation of Carcinogenic Risks to Humans, Vol 106. Some Chlorinated Solvents and Their Metabolites. International Agency for Research on Cancer, Lyon.
IARC, 2011. Permeable Reactive Barrier: Technology Update. The Interstate Technology & Regulatory Council. PRB-5, 26-40. Interstate Technology & Regulatory Council, PRB: Technology Update Team, Washington, D.C.. https://itrcweb.org/teams/projects/permeable-reactive-barriers. (Accessed 15 September 2024)
Kim, Y., Carraway, E.R., 2003. Reductive dechlorination of TCE by zero valent bimetals. Environ. Technol. 24, 69–75. https://doi.org/10.1080/09593330309385537.
Lang, Y., Yu, Y., Zou, H., Ye, J., Zhang, S., 2022. Performance and mechanisms of sulfidated nanoscale zero-valent iron materials for toxic TCE removal from the groundwater. Int. J. Environ. Res. Publ. Health 19, 6299. https://doi.org/10.3390/ijerph19106299.
Liu, J., Zhu, H., Xu, F., Zhao, J., 2017. Enhanced hydrodechlorination of 4-chlorophenol by Cu/Fe bimetallic system via ball-milling. Desalination Water Treat. 64, 157–164. https://doi.org/10.5004/dwt.2017.20171.
Liu, Y., Majetich, S.A., Tilton, R.D., Sholl, D.S., Lowry, G.V., 2005. TCE dechlorination rates, pathways, and efficiency of nanoscale iron particles with different properties. Environ. Sci. Technol. 39, 1338–1345. https://doi.org/10.1021/es049195r.
Ma, J., McHugh, T., Beckley, L., Lahvis, M., DeVaull, G., Jiang, L., 2020. Vapor intrusion investigations and decision-making: a critical review. Environ. Sci. Technol. 54, 7050–7069. https://doi.org/10.1021/acs.est.0c00225.
Mahmoodlu, M.G., Hassanizadeh, S.M., Hartog, N., Raoof, A., 2014. Oxidation of trichloroethylene, toluene, and ethanol vapors by a partially saturated permeable reactive barrier. J. Contam. Hydrol. 164, 193–208. https://doi.org/10.1016/j.jconhyd.2014.05.013.
Mahmoodlu, M.G., Hassanizadeh, S.M., Hartog, N., Raoof, A., Van Genuchten, M.Th, 2015. Evaluation of a horizontal permeable reactive barrier for preventing upward diffusion of volatile organic compounds through the unsaturated zone. J. Environ. Manag. 163, 204–213. https://doi.org/10.1016/j.jenvman.2015.08.025.
Mangayayam, M., Dideriksen, K., Ceccato, M., Tobler, D.J., 2019. The structure of sulfidized zero-valent iron by one-pot synthesis: impact on contaminant selectivity and long-term performance. Environ. Sci. Technol. 53, 4389–4396. https://doi.org/10.1021/acs.est.8b06480.
Massmann, J., Farrier, D.F., 1992. Effects of atmospheric pressures on gas transport in the vadose zone. Water Resour. Res. 28, 777–791. https://doi.org/10.1029/91WR02766.
McCarty, P.L., 2010. Groundwater contamination by chlorinated solvents: history, remediation Technologies and strategies. In: Stroo, H.F., Ward, C.H. (Eds.), In Situ Remediation of Chlorinated Solvent Plumes, SERDP/ESTCP Environmental Remediation Technology. Springer, New York, New York, NY, pp. 1–28. https://doi.org/10.1007/978-1-4419-1401-9_1.
McHugh, T.E., McAlary, T., 2009. Important physical processes for vapor intrusion: a literature review. In: Proceedings of AWMA Vapor Intrusion Conference.
Mo, Y., Xu, J., Zhu, L., 2022. Molecular structure and sulfur content affect reductive dechlorination of chlorinated ethenes by sulfidized nanoscale zerovalent iron. Environ. Sci. Technol. 56, 5808–5819. https://doi.org/10.1021/acs.est.2c00284.
O'Carroll, D., Sleep, B., Krol, M., Boparai, H., Kocur, C., 2013. Nanoscale zero valent iron and bimetallic particles for contaminated site remediation. Adv. Water Resour. 51, 104–122. https://doi.org/10.1016/j.advwatres.2012.02.005.
Phillips, D.H., Nooten, T.V., Bastiaens, L., Russell, M.I., Dickson, K., Plant, S., Ahad, J.M. E., Newton, T., Elliot, T., Kalin, R.M., 2010. Ten year performance evaluation of a field-scale zero-valent iron permeable reactive barrier installed to remediate trichloroethene contaminated groundwater. Environ. Sci. Technol. 44, 3861–3869. https://doi.org/10.1021/es902737t.
Qian, L., Li, H., Wei, Z., Liang, C., Dong, X., Lin, D., Chen, M., 2023. Enhanced removal of cis-1,2-dichloroethene and vinyl chloride in groundwater using ball-milled sulfur- and biochar-modified zero-valent iron: from the laboratory to the field. Environ. Pollut. 336, 122424. https://doi.org/10.1016/j.envpol.2023.122424.
Qu, M., Chen, H., Wang, Y., Wang, X., Tong, X., Li, S., Xu, H., 2021. Improved performance and applicability of copper-iron bimetal by sulfidation for Cr(VI) removal. Chemosphere 281, 130820. https://doi.org/10.1016/j.chemosphere.2021.130820.
Rajajayavel, S.R.C., Ghoshal, S., 2015. Enhanced reductive dechlorination of trichloroethylene by sulfidated nanoscale zerovalent iron. Water Res. 78, 144–153. https://doi.org/10.1016/j.watres.2015.04.009.
Ruan, X., Liu, H., Wang, J., Zhao, D., Fan, X., 2019. A new insight into the main mechanism of 2,4-dichlorophenol dechlorination by Fe/Ni nanoparticles. Sci. Total Environ. 697, 133996. https://doi.org/10.1016/j.scitotenv.2019.133996.
Scaria, J., Nidheesh, P.V., Kumar, M.S., 2020. Synthesis and applications of various bimetallic nanomaterials in water and wastewater treatment. J. Environ. Manag. 259, 110011. https://doi.org/10.1016/j.jenvman.2019.110011.
Schrick, B., Blough, J.L., Jones, A.D., Mallouk, T.E., 2002. Hydrodechlorination of trichloroethylene to hydrocarbons using bimetallic Nickel−Iron nanoparticles. Chem. Mater. 14, 5140–5147. https://doi.org/10.1021/cm020737i.
Settimi, C., Zingaretti, D., Sanna, S., Verginelli, I., Luisetto, I., Tebano, A., Baciocchi, R., 2022. Synthesis and characterization of zero-valent Fe-Cu and Fe-Ni bimetals for the dehalogenation of trichloroethylene vapors. Sustainability 14, 7760. https://doi.org/10.3390/su14137760.
Settimi, C., Zingaretti, D., Verginelli, I., Baciocchi, R., 2023. Degradation of trichloroethylene vapors by micrometric zero-valent Fe Cu and Fe Ni bimetals under partially saturated conditions. J. Contam. Hydrol. 257, 104204. https://doi.org/10.1016/j.jconhyd.2023.104204.
Sun, Y., Zheng, K., Du, X., Qin, H., Guan, X., 2024. Insights into the contrasting effects of sulfidation on dechlorination of chlorinated aliphatic hydrocarbons by zero-valent iron. Water Res. 255, 121494. https://doi.org/10.1016/j.watres.2024.121494.
Tian, F., Tang, J., Zeng, J., Luo, Z., Zhang, L., Tang, F., Han, Z., Yang, X., 2022. Degradation of atrazine by Ni-doped sulfidated microscale zero-valent iron: mechanistic insights for enhanced reactivity and selectivity. Chem. Eng. J. 435, 135120. https://doi.org/10.1016/j.cej.2022.135120.
Venkateshaiah, A., Silvestri, D., Wacławek, S., Ramakrishnan, R.K., Krawczyk, K., Saravanan, P., Pawlyta, M., Padil, V.V.T., Černík, M., Dionysiou, D.D., 2022. A comparative study of the degradation efficiency of chlorinated organic compounds by bimetallic zero-valent iron nanoparticles. Environ. Sci. Water Res. Technol. 8, 162–172. https://doi.org/10.1039/d1ew00791b.
Verginelli, I., Capobianco, O., Hartog, N., Baciocchi, R., 2017. Analytical model for the design of in situ horizontal permeable reactive barriers (HPRBs) for the mitigation of chlorinated solvent vapors in the unsaturated zone. J. Contam. Hydrol. 197, 50–61. https://doi.org/10.1016/j.jconhyd.2016.12.010.
Verginelli, I., Yao, Y., 2021. A review of recent vapor intrusion modeling work. Groundw. Monit. Remediat. 41, 138–144. https://doi.org/10.1111/gwmr.12455.
Wang, S., Song, L., He, H., Zhang, W., 2024. A two-dimensional analytical model for volatile organic compound diffusion through the unsaturated soil and horizontal permeable reactive barriers. Water Air Soil Pollut. 235, 414. https://doi.org/10.1007/s11270-024-07211-4.
Wang, Z., Zhang, Y., Li, F., Han, H., Xu, C., 2022. Reaching beyond the sulfided surface: doping of copper cation to expand the pH tolerance range for SZVI. Chem. Eng. J. 429, 132161. https://doi.org/10.1016/j.cej.2021.132161.
Wu, S., Cai, S., Qin, F., He, F., Liu, T., Yan, X., Wang, Z., 2023. Reductive dechlorination of chlorinated ethenes by ball milled and mechanochemically sulfidated microscale zero valent iron: a comparative study. J. Hazard Mater. 446, 130730. https://doi.org/10.1016/j.jhazmat.2023.130730.
Xiao, S., Jin, Z., Dong, H., Xiao, J., Li, Y., Li, L., Li, R., Chen, J., Tian, R., Xie, Q., 2022. A comparative study on the physicochemical properties, reactivity and long-term performance of sulfidized nanoscale zerovalent iron synthesized with different kinds of sulfur precursors and procedures in simulated groundwater. Water Res. 212, 118097. https://doi.org/10.1016/j.watres.2022.118097.
Xu, F., Deng, S., Xu, J., Zhang, W., Wu, M., Wang, B., Huang, J., Yu, G., 2012. Highly active and stable Ni–Fe bimetal prepared by ball milling for catalytic hydrodechlorination of 4-chlorophenol. Environ. Sci. Technol. 46, 4576–4582. https://doi.org/10.1021/es203876e.
Xu, J., Avellan, A., Li, H., Liu, X., Noël, V., Lou, Z., Wang, Y., Kaegi, R., Henkelman, G., Lowry, G.V., 2020. Sulfur loading and speciation control the hydrophobicity, electron transfer, reactivity, and selectivity of sulfidized nanoscale zerovalent iron. Adv. Mater. 32, 1906910. https://doi.org/10.1002/adma.201906910.
Xu, J., Wang, Y., Weng, C., Bai, W., Jiao, Y., Kaegi, R., Lowry, G.V., 2019. Reactivity, selectivity, and long-term performance of sulfidized nanoscale zerovalent iron with different properties. Environ. Sci. Technol. 53, 5936–5945. https://doi.org/10.1021/acs.est.9b00511.
Xu, W., Xia, C., He, F., Wang, Z., Liang, L., 2024. Sulfidation of nanoscale zero-valent iron by sulfide: the dynamic process, mechanism, and role of ferrous iron. Environ. Sci. Technol. https://doi.org/10.1021/acs.est.4c04390.
Yan, Z., Ouyang, J., Wu, B., Liu, C., Wang, H., Wang, A., Li, Z., 2024. Nonmetallic modified zero-valent iron for remediating halogenated organic compounds and heavy metals: a comprehensive review. Environ. Sci. Ecotechnol. 21, 100417. https://doi.org/10.1016/j.ese.2024.100417.
Yang, Z., Ding, G., Yan, L., Wang, R., Zhang, W., Wang, X., Rao, P., 2023. Ball-milled sulfide iron-copper bimetals based composite permeable materials for Cr (VI) removal: effects of preparation parameters and kinetics study. Chemosphere 338, 139388. https://doi.org/10.1016/j.chemosphere.2023.139388.
Yao, Y., Shen, R., Pennell, K.G., Suuberg, E.M., 2013. A review of vapor intrusion models. Environ. Sci. Technol. 47, 2457–2470. https://doi.org/10.1021/es302714g.
You, K., Zhan, H., 2013. Comparisons of diffusive and advective fluxes of gas phase volatile organic compounds (VOCs) in unsaturated zones under natural conditions. Adv. Water Resour. 52, 221–231. https://doi.org/10.1016/j.advwatres.2012.11.021.
Zhang, Y., Ozcer, P., Ghoshal, S., 2021. A comprehensive assessment of the degradation of C1 and C2 chlorinated hydrocarbons by sulfidated nanoscale zerovalent iron. Water Res. 201, 117328. https://doi.org/10.1016/j.watres.2021.117328.
Zhu, Z.-W., Feng, S.-J., Zheng, Q.-T., Chen, H.-X., Wei, H., 2024. Analytical model for the mitigation of VOC vapor with horizontal permeable reactive barrier in the contaminated site considering non-uniform source. Sci. Total Environ. 948, 174746. https://doi.org/10.1016/j.scitotenv.2024.174746.
Zingaretti, D., Verginelli, I., Baciocchi, R., 2019. Dehalogenation of trichloroethylene vapors by partially saturated zero-valent iron. Sci. Total Environ. 647, 682–689. https://doi.org/10.1016/j.scitotenv.2018.08.011.
Zingaretti, D., Verginelli, I., Luisetto, I., Baciocchi, R., 2020. Horizontal permeable reactive barriers with zero-valent iron for preventing upward diffusion of chlorinated solvent vapors in the unsaturated zone. J. Contam. Hydrol. 234, 103687. https://doi.org/10.1016/j.jconhyd.2020.103687.
Zou, H., Hu, E., Yang, S., Gong, L., He, F., 2019. Chromium(VI) removal by mechanochemically sulfidated zero valent iron and its effect on dechlorination of trichloroethene as a co-contaminant. Sci. Total Environ. 650, 419–426. https://doi.org/10.1016/j.scitotenv.2018.09.003.